

# AC Conductivity of GeSe<sub>5</sub> Chalcogenide Glasses

A. Abdallah\*

Physics Department, Faculty of Science, Ain Shams University,  
Abbassia, 11556 Cairo, Egypt.

*Ac conductivity and dielectric properties of bulk GeSe<sub>5</sub> semiconducting glasses were studied in the frequency and temperature range of 50 Hz-5 MHz and 303-483 K, respectively. The XRD confirmed the amorphous nature of GeSe<sub>5</sub> semiconducting glasses. Ac conductivity,  $\sigma_{ac}(\omega)$ , as a function of frequency varies as a power law:  $\sigma_{ac}(\omega) = A\omega^{\delta}$ . Temperature dependence of frequency exponent was analyzed to predict the conduction mechanism, which was found to be correlated barrier hopping model (CBH). Frequency and temperature dependences of dielectric constant and dielectric loss were also investigated. Electric modulus formalism was applied for evaluating the activation energy of the dielectric relaxation process.*

## 1. Introduction

Chalcogenide glass (CGs) meaning glass has one or more chalcogene element like (S, Se, Te) [1-7]. CGs are amorphous semiconductor, amorphous due to short range order and soft semiconductor due to flexible atomic structure. It also has band gap energy  $\sim 2$  eV, where semiconductor materials have band gap 1-3 eV. Chalcogenide glasses have many promising applications [8] in civil, military, and medical [9]. It has also many promising application in electronic devices and electronic switches [10]. CGs has good optical properties like photoinduced phenomena "heat-mode, photon mode phenomena [11, 12].

The binary compounds GeSe is characterized by highly anisotropic properties due to their layered structure. The interaction between layers is very weak, due to van der Waals force. It is established that the physical properties of this system are highly composition dependent [13]. The glass formation region in the binary Ge-Se system is about 60-90 at% Se, with rest being Ge [14]. GeSe chalcogenide glasses were studied by many authors [13-21]. Pan et al, studied the annealing effects on the structure and optical properties of GeSe<sub>2</sub> and GeSe<sub>4</sub> [15]. Petkov studied amorphous chalcogenide Ge-Se-(Ba, Ga, TI) glasses and thin films, their preparation, properties and application [16]. Jemali et al, calculated ab

initio of vibrational frequencies of  $\text{GeSe}_3$  and  $\text{GeSe}_4$  [17]. While, Popov et al, has studied thin amorphous chalcogenide glasses films of  $(\text{GeSe}_4)_{100-x}\text{Ga}_y$  and  $(\text{GeSe})_{100-y}\text{Ga}(\text{Ti}, \text{B})_y$  ( $y = 5, 10, 15, 20$ ) system and their internal stress using cantilever technique [18]. Boudebs et al, reported the linear optical properties of  $\text{GeSe}_4$  with other composition as chalcogenide glasses near infrared range [19]. Nedeva et al, investigated bulk and thin films of  $(\text{GeSe}_4)_{1-x}\text{Ga}_x$  and  $(\text{GeSe}_5)_{1-x}\text{Ga}_x$  systems with up to 20 at % Ga. They investigated the compositional dependence of the optical properties [20]. Dwivedi et al, studied the change in bonding configurations for  $\text{GeSe}_4$  films exposed to visible light and irradiated with Krypton ions by using Raman techniques [21]. There is no detailed study on the ac conductivity of  $\text{GeSe}_5$  glasses. Therefore, it is interesting to study the ac conductivity and dielectric properties of  $\text{GeSe}_5$  chalcogenide glasses and the effect of frequency and temperature which may give insight for its application.

## 2. Experimental Technique

$\text{GeSe}_5$  amorphous Chalcogenide was prepared by weighting appropriate amounts of high purity element (5 N) and putting them in quartz ampoule sealed under pressures of  $\sim 1.3 \times 10^{-3}$  Pa. The quartz ampoule was heated to 1173 K for 24 hours. The molten was then quenched in icy water. The composition and homogeneity of  $\text{GeSe}_5$  glasses was checked using the energy dispersive X-ray analysis (EDX) attached to the scanning electron microscope SEM Model Quanta 250 FEG FEI company, Netherlands. The X-ray diffraction (XRD) study was performed using Philips X'pert diffractometer using  $\text{CuK}_\alpha$  radiation.  $\text{GeSe}_5$  bulk was ground to obtain fine powder; the powder was pressed in the form of pellet of diameter  $1.3 \times 10^{-2}$  m and thickness  $1.05 \times 10^{-3}$  m. Au thin film was deposited on the opposite sides of pellet as ohmic electrodes using Edward 306A thermal evaporation unit under vacuum of  $\sim 1.33 \times 10^{-4}$  Pa. The dielectric measurements were carried out using programmable LCR bridge Tgan INC. 3350 in the frequency range 50 Hz -5 MHz and in temperature range 303-483 K. The temperature was measured using Chromel-Alumel thermocouple. The accuracy in the measurement of dielectric constant is  $\pm 1 \times 10^{-3}$  and for loss is  $\pm 1 \times 10^{-4}$ .

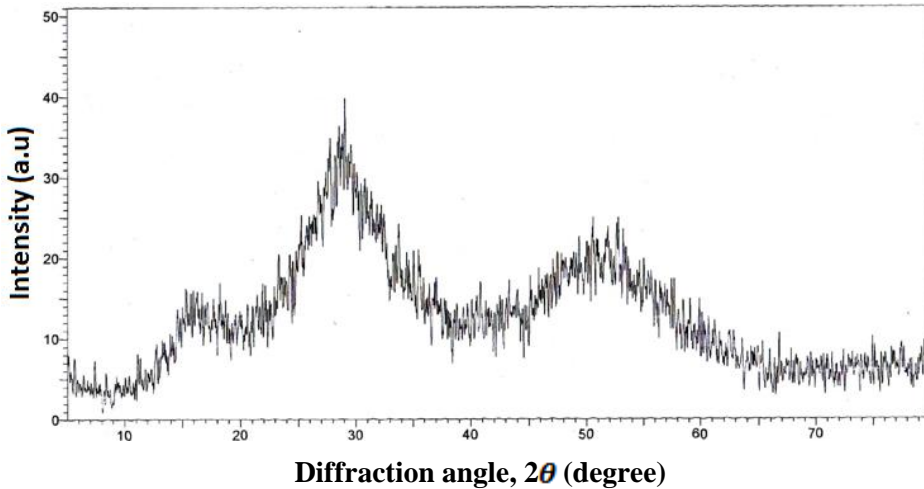
## 3. Result and Discussion

The X-ray diffraction pattern of  $\text{GeSe}_5$  is shown in Fig. (1 a). The diffraction pattern confirms the amorphous nature of  $\text{GeSe}_5$  chalcogenide glasses. Figure 1.b. shows the EDX of amorphous  $\text{GeSe}_5$  which confirms the agreement between the experimental atomic ratio of the element and the expected data.

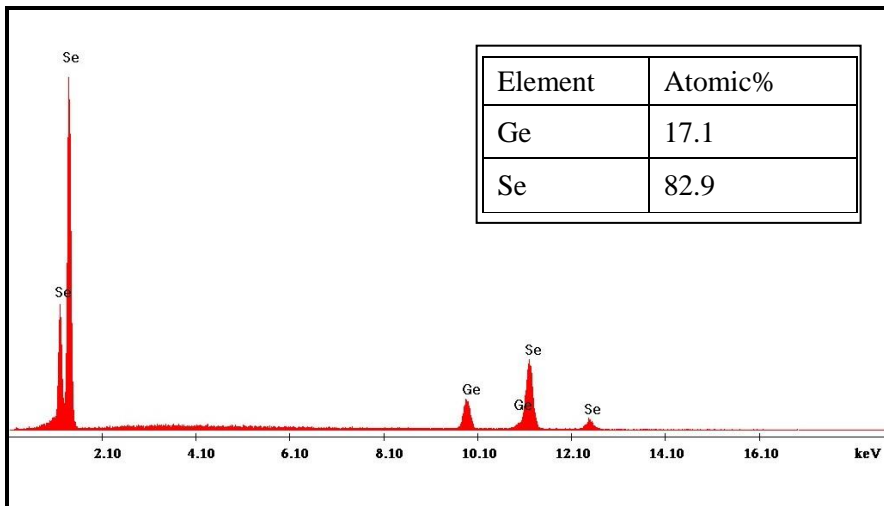
### 3.1 Frequency and Temperature dependence of $\sigma_{ac}(\omega)$

The total conductivity ( $\sigma_{tot}(\omega)$ ) is a sum of two components; dc conductivity ( $\sigma_{dc}$ ) which is frequency independent and the ac conductivity which is frequency dependent according to the relation  $\sigma_{ac}(\omega) = A\omega^s$  [22, 23]. Where A is a constant dependent on temperature, ( $\omega$ ) is the angular frequency and s is the frequency exponent. Therefore,

$$\sigma_{ac}(\omega) = \sigma_{tot}(\omega) - \sigma_{dc} = A\omega^s \tag{1}$$



(a)



(b)

**Fig. (1)**

Figure (2) shows the frequency dependence of the ac conductivity ( $\sigma_{ac}$ ) at different temperatures. It is clear that the  $\sigma_{ac}(\omega)$  increases with increasing frequency and temperatures. The frequency exponent ( $s$ ) was determined from the linear fit of the straight lines at different temperatures. The exponent was found to be less than unity and decreases with increasing temperatures. Figure 3 shows the dependence of the frequency exponent  $s$  on temperature. This result suggests that the correlated barrier hopping (CBH) model is the suitable model to describe the ac conductivity. According to this model, charge carriers are supposed to hop between neighboring localized sites. The dependence of the frequency exponent  $s$  on temperature is given by the relation:

$$1 - s = \frac{6KT}{W} \quad (2)$$

where,  $K$  is Boltzmann constant and  $W$  is the maximum barrier height.

The maximum barrier height can be obtained from fitting the data shown in Fig (3). Two straight lines were obtained with slope  $s_1$  at  $T < 400$  K and  $s_2$  at  $T > 400$  K. The maximum barrier height obtained is 0.420 eV and 0.761 at lower ( $T < 400$  K) and higher temperatures ( $T > 400$  K), respectively.

The temperature dependence of the ac conductivity at different constant frequency for GeSe<sub>5</sub> semiconductor is shown in Fig. (4). It is clear that this dependence is Arrhenius relation according to the relation

$$\sigma_{ac} = \sigma_o \exp \frac{\Delta E_{ac}}{KT} \quad (3)$$

where,  $\sigma_o$  is the pre-exponential factor and  $\Delta E_{ac}$  is the ac conductivity activation energy. This figure show that ac conductivity increases with increasing temperature. According to the Arrhenius relation, the ac conductivity is thermally activated from different localized states in the gap or its tail [24, 25].

The dependence of the ac activation energy on the frequency was calculated from the slope of the linear fit of the lines. Fig. (5), shows the dependence of the ac activation energy ( $\Delta E_{ac}$ ) on the frequency. The values of  $\Delta E_{ac}$  was found to decrease with increasing frequency. This is due to that increasing frequency enhances the electronic jumps between localized states, which consequently decrease the ac activation energy ( $\Delta E_{ac}$ ) [26, 27].

### 3.2. DC conductivity as a function of temperature

DC conductivity ( $\sigma_{dc}$ ) was obtained from the extrapolation of ( $\sigma_{tot}(\omega)$ ) to  $\omega = 0$ . Figure 6 shows the temperature dependence for  $\sigma_{dc}T$ . It is clear that

the dc conductivity ( $\sigma_{dc}$ ) decreases with increasing the temperature according to the relation [28]:

$$\sigma_{dc} = (\sigma_o/T) \exp\left(\frac{-\Delta E_{dc}}{KT}\right) \tag{4}$$

where,  $\Delta E_{dc}$  is the activation energy for dc conductivity and  $K$  is the Boltzmann's constant. The values of the dc conductivity activation energy were calculated from the slope of the linear fit. The activation energy for the dc conductivity was found to be 0.398 and 0.761 eV at lower ( $T < 400$  K) and higher ( $T > 400$  K) temperature, respectively.

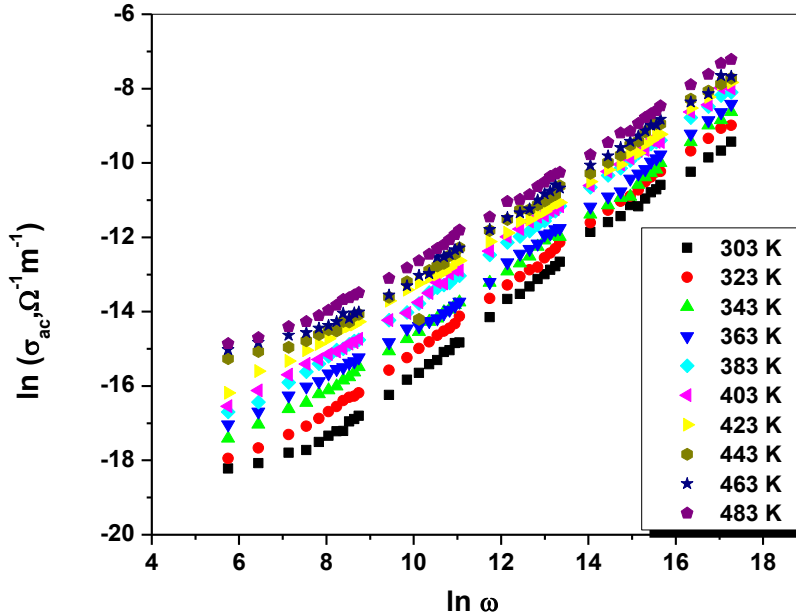


Fig. (2)

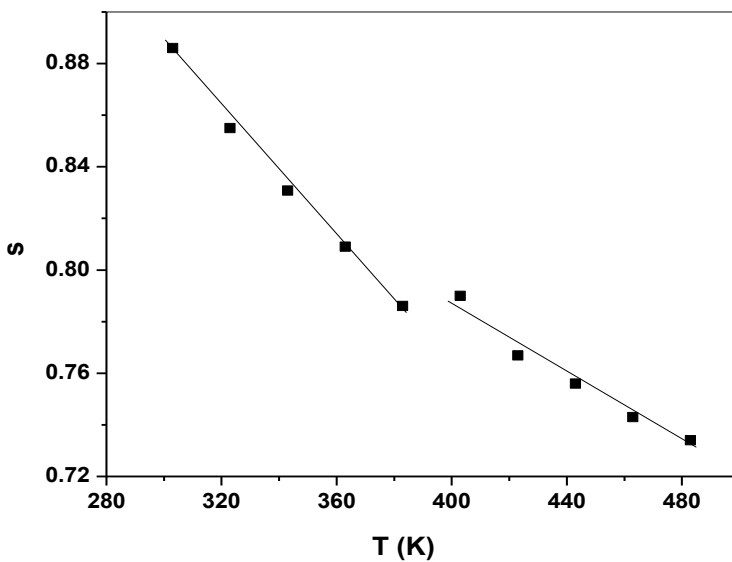


Fig. (3)

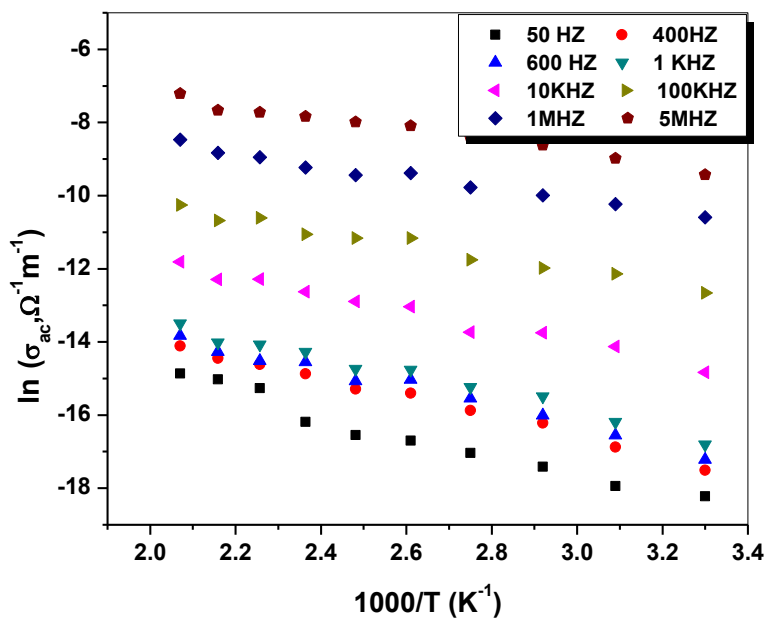


Fig. (4)

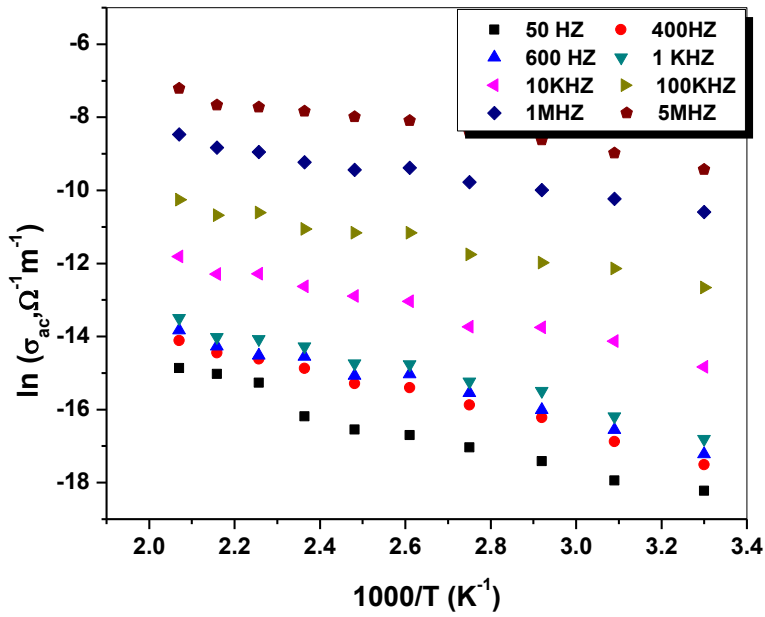


Fig. (4)

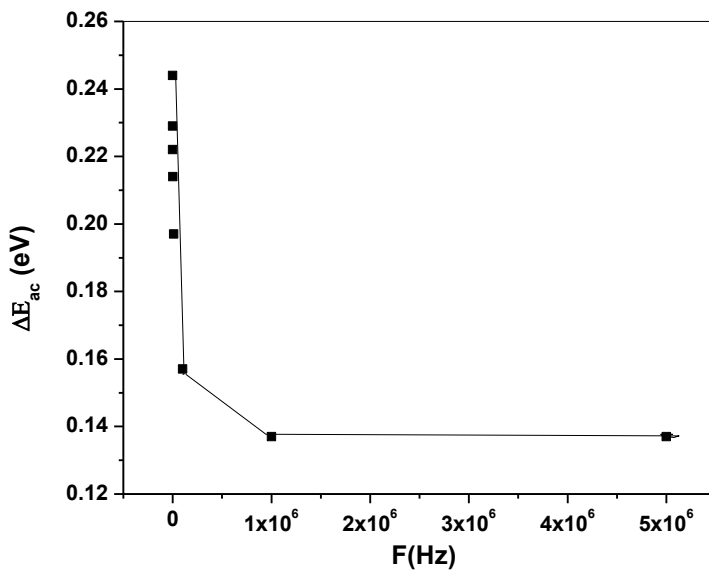


Fig. (5)

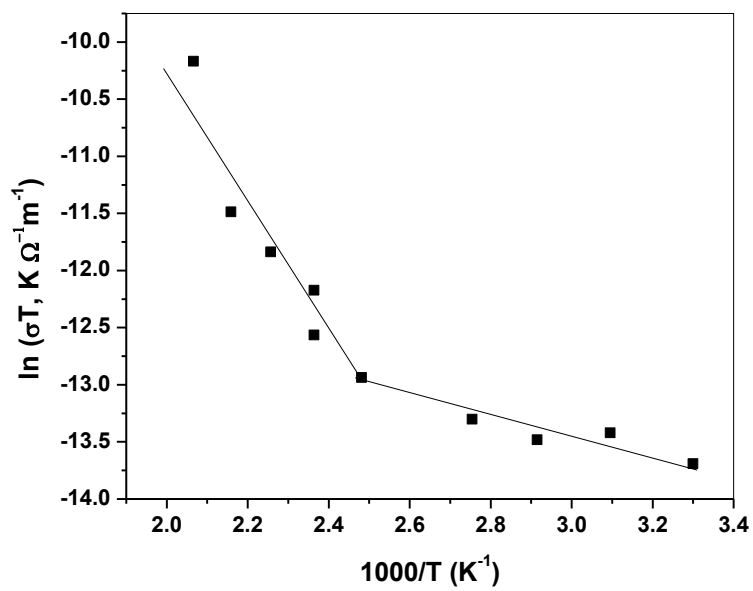


Fig. (6)

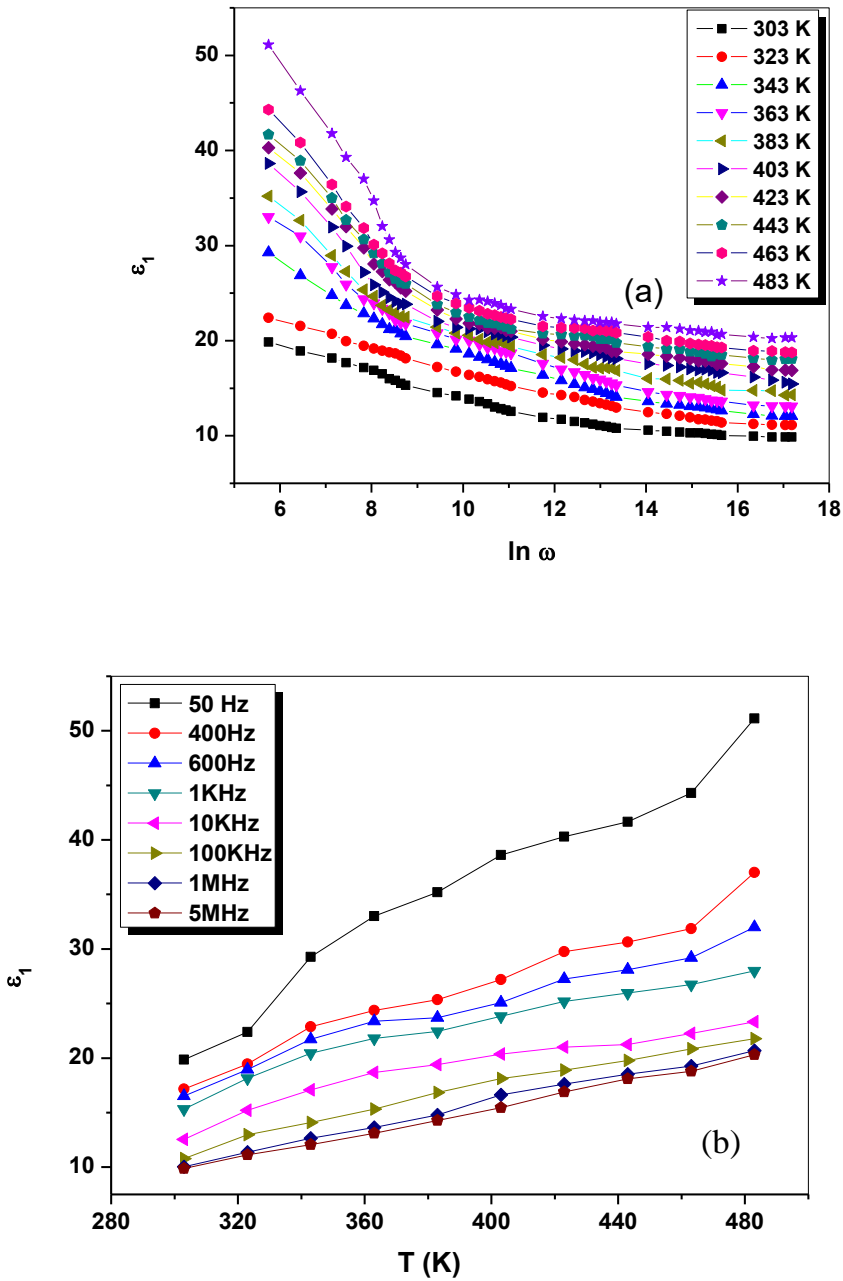


Fig. (7)

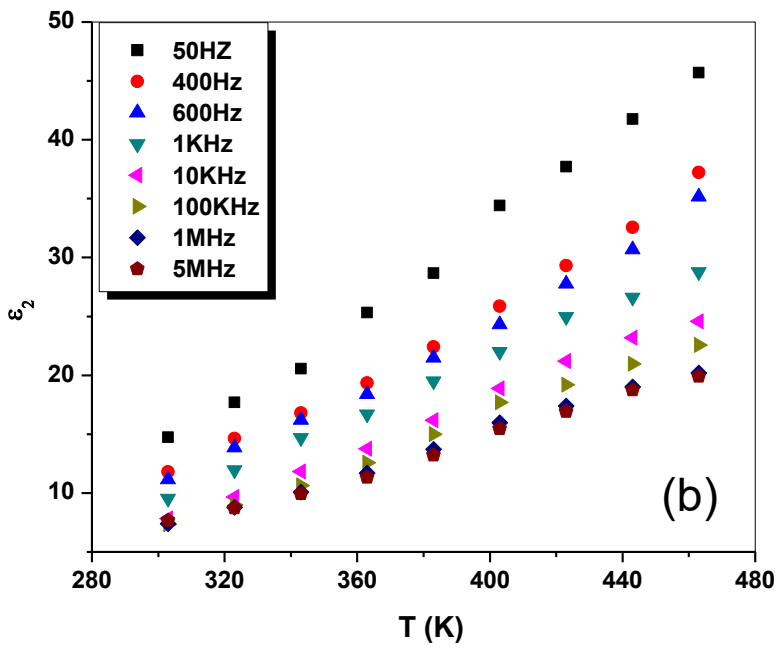
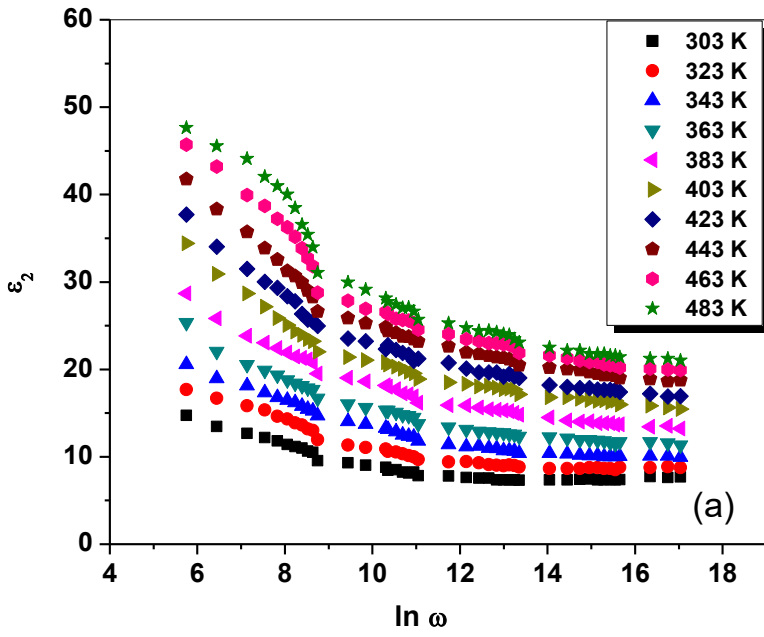


Fig. (8)

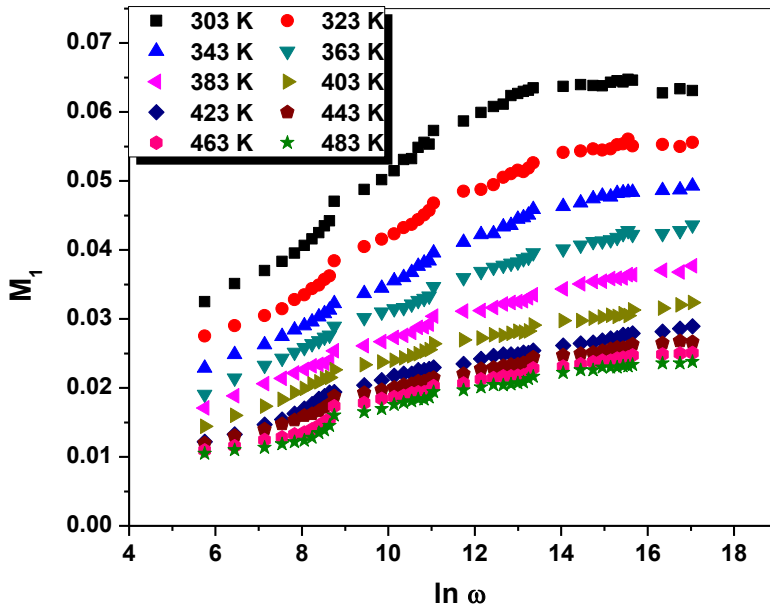


Fig. (9)

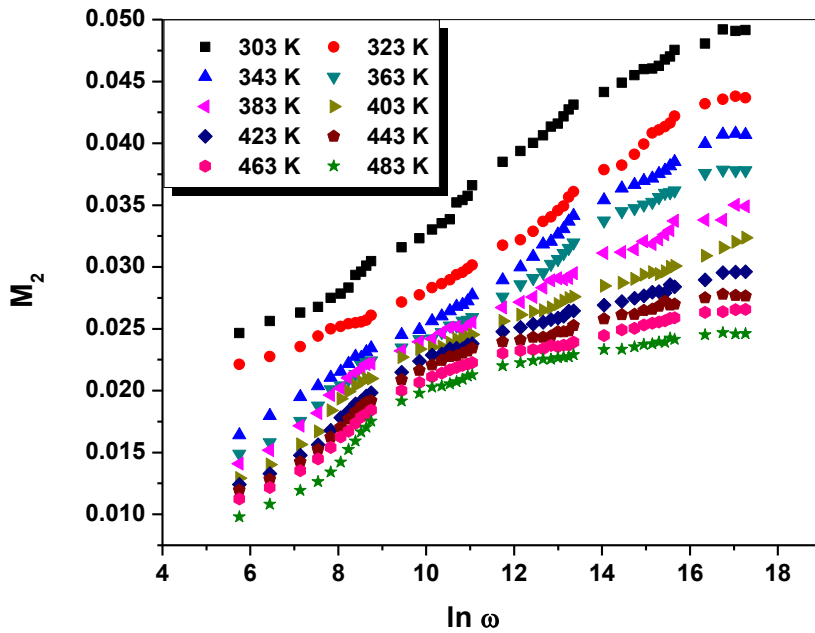


Fig (10)

### 3.3. Dielectric properties: Frequency and temperature dependence of the dielectric constant and dielectric loss

The dielectric constant  $\epsilon_1$  can be calculated using the relation  $\epsilon_1 = \frac{dc}{A\epsilon_0}$ , where  $c$  is the sample capacitance,  $d$  is the sample thickness,  $A$  is the cross sectional area and  $\epsilon_0$  is the permittivity of free space. Figure 7 (a, b) shows the dependence of the dielectric constant with frequency and temperature.

Figure 7-a show that  $\epsilon_1$  decrease with increasing frequency. This can be attributed to that polarization of the dielectric material is due to the contribution of four polarizations [29]. This is related to the dielectric constant. These are electronic, ionic, orientation and space charge. With increasing frequency, the orientation polarization decreases since, the dipoles cannot be able to rotate sufficiently rapidly, so their oscillation lag behind the field .With further increase of frequency, the dipole will be unable to follow the field and the orientation polarization stopped. Therefore  $\epsilon_1$  decrease to a constant value due to space charge polarization at higher frequencies.

Figure 7-b shows the increase of  $\epsilon_1$  with increasing temperature. This can attributed to that at low temperatures the dipole cannot orient themselves. Then with increasing the temperature the orientation polarization increases with the increase of  $\epsilon_1$  [30].

The dielectric loss can be calculated from the relation

$$\epsilon_2 = \epsilon_1 \tan \delta \quad (5)$$

Figure 8-a show that  $\epsilon_2$  decrease with increasing frequency. At low frequencies,  $\epsilon_2$  is due to ions migration in the material. At moderate frequencies,  $\epsilon_2$  is due to contribution of ions jump, conduction loss of ions migration, and ion polarization loss. While, at higher frequencies the only source of dielectric loss is the ion vibration and  $\epsilon_2$  has minimum value [30, 31].

Figure 8-b shows the dependence of  $\epsilon_2$  with increasing temperature. This can be explained according to Stevels [30]. The relaxation phenomenon is divided into conduction loss, dipole loss and vibration loss. At lower temperatures, the conduction loss is minimum because it is proportional to  $\sigma(\omega)$ . With increasing temperatures,  $\sigma$  increases and consequently the conduction loss increases which lead to increase  $\epsilon_2$  with increasing temperature. It is also clear from this figure that  $\epsilon_2$  decrease with increasing frequency. At low frequencies,  $\epsilon_2$  is due to ions migration in the material. At moderate frequencies,  $\epsilon_2$  is due to contribution of ions jump, conduction loss of ions migration, and ion polarization loss. While, at higher frequencies the only source of dielectric loss is the ion vibration and  $\epsilon_2$  has minimum value. The reported values of  $\epsilon_2$  are in agreement with that reported in literature [32, 33].

Relaxation mechanism can be obtained from the electric modulus study [34]. The electric modulus is represented by:

$$M^* = 1/\epsilon^*(\omega) \quad (6)$$

$$M^* = M_1(\omega) + M_2(\omega) \quad (7)$$

where, the real and imaginary parts  $M_1$  and  $M_2$  of the dielectric modulus are:

$$M_1 = \epsilon_1 / [(\epsilon_1)^2 + (\epsilon_2)^2] \quad (8)$$

$$M_2 = \varepsilon_2 / [(\varepsilon_1)^2 + (\varepsilon_2)^2] \quad (9)$$

From figure 9 and figure 10 which show the real and imaginary part of modulus, we conclude that this value for the dielectric modulus increase with increasing frequency and decrease with increasing temperature. This suggests that the range in which charge carriers are mobile on long distances i.e. polaron can perform successful hopping from one site to the neighboring site. The absence of the peak of the imaginary part is observed in literature [35].

### Conclusion

X-ray diffraction analysis confirmed the amorphous nature of GeSe<sub>5</sub> chalcogenide glasses. Ac conductivity varies with  $\omega^s$ . The temperature dependence of the exponent  $s$  supports the correlated barrier hopping model as the predominant ac conduction mechanism. The temperature dependence of ac conductivity shows a linear increase with increasing temperature with activation energy of relaxation process 0.708 eV. Both dielectric constant and dielectric loss of GeSe<sub>5</sub> glasses decreased with increasing frequency over the investigated frequency range 50 Hz- 5 MHz. The real and imaginary parts of electric modulus were also investigated.

### References

1. A.R. Barik, Ramakanta Nail, K.V. Adarsh, J. Non-Cryst. Solids 377 (2013) 179.
2. M.T. Kostyshin, E.V. Mikhailovskaya, P.F Romanenok, Sov. Phys. Solid State 8 (1966) 451.
3. A. Zakery, S.R. Elliot, J. Non-Cryst. Solids 1 (2003) 330.
4. A. Canjoo., K. Shimkawa, K. Kitano, E.A. Davis, J. Non-Cryst. Solids 917 (2002) 2990.
5. A. Canjoo, N. Yoshida, K. Shimkawa, in: M. Kawasaki, N. Ashrigitz, R. Anthony (Eds), Recent Research Devolvment in Applied Physics, 2, Research Signpot. Trivandrum, (1999) 129.
6. R. Ferichs, Phys. Rev. 78 (1950) 643.
7. R. Ferichs, J.Opt. Soc. B 43 (1953) 1153.
8. N. Mehta, Journal of Scientific and Industrial Research, 65 (2006) 777.
9. Jun Bin Ko and Tea –Sik Myung, J. of Ceramic Processing Reaserch 12, (2011) 132.
10. A.M.A. El Barry, H.E. Atyia, Physica B 368 (2005) 1.
- 11- A.Zakery, S.R.Elliot, J.Non-cryst. Solids 1 (2003) 330.
12. K. Shimakaw, A. Kolobov and S.R. Elliot, Adv. Phys. 44 (1995) 475.
13. A.A Othman, K.A. Aly, A.M. Abousehly. Thin Solid Films 515 (2007) 507.
14. Z.U. Borisova, Glassy Semiconductors, Pelunum Press, New York, 1981.
15. R.K. Pan, H.Z. Tao, H.C. Zang, X.J. Zhao, T.J. Zhang, J. of Alloy and Compounds 484 (2009) 645.

16. P. Petkov, *Nanostructured Materials For Advanced Technological Applications*, Springer Science + Business Media B.V. (2009).
17. N.A. Jemali, H.A. Kassim, V. R. Devi, K.N. Shrivastva, , *J. Non-Cryst. Solids* 354 (2008) 1744.
18. C. Popov, S. Boycheva, P. Petkov, Y. Nedeva, B. Monchev, S. Parvanov, *Thin Solid Films* 496 (2006) 718.
19. G. Boudebs, S. Cherukulappurath, M. Guignard, J. Troles, F. Smekta, F. Sanchez, *Communications* 230 (2004) 331.
20. Y. Nedeva, T. Petkova, E. Mytilineou, P. Petkov, *J. Optoelectronics and Materials* 3 (2001) 433.
21. P.K. Dwivedi, S.K. Tripathi, A. Pradhan, V.N. Kulkarni, S.C. Agarwal, *J. Non-Cryst. Solids* 266-269 (2000) 924.
22. S.R. Elliot, *Physics of Amorphous Material*, Willey, New York, (1983).
23. N.F. Mott, E.A. Davis, *Electronic Process in Non-Cryst Materials*, Clarendon Press, Oxford, 1979.
  
24. N. A. Hegab, A. E. Bekheet, M. A. Afifi, L. A. Wahaba, H. A. Shehata  
*Journal Ovonic Research* 3( 2007) 71.
25. M.M. El-Nahass, A.M. Farid, K.F. Abd El-Rahman, H.A.M. Ali, *Physica B* 03 (2008) 2331.
  
26. A.A.A. Darwish, M.M. El-Nahass, A.E. Bekheet, *J. Alloys Compd.*, 586 (2014) 142.
  
27. M.M. El-Nahass, H.A.M. Ali, E.F.M. El-zaidia , *Physica B* 431 (2013) 52.
28. T. Sankarappa, M. Prashant Kumar, G.B. Devidas, N. Nagaraja, R. Rama Ramakrishnareddy, *Journal of Molecular structure* 889 (2008) 308-315.
29. B.S. Patial, Neha, J. Prakash, R. Kumar, S.K. Tripathi, N. Thakur, *Journal Of Nano-And Electronic Physics*,5 (2013) 2019.
  
30. J.M. Stevels, *Handbuck der physik*, (1975) 350.
  
31. F. Salman, *Turk J Phys*, 28 (2004) 41.
32. M.M. El-Nahass, A.F. El-Deeb, El-Sayed, A.M. Hassaniem, *Physica B* 388 (2007) 26-33.
33. A. KUMAR, M.LAL, K. SHARMA, P.S.GILL, NAVDEEPGOYAL, *Chalcogenide letter* Vol. 11, No. 5, May 2014, p. 249 – 256.
  
34. M. Haj Lakhdar, B. OUNI, M. Amlouk, *Materials Science in Semiconductor Processing* 19 (2014) 32.

35.N. Kishore, Sanjay, A. Agarwal, Sanjay Dahiya, Inder Pal, Int. Conf. on Materials Science and Technology (ICMST 2012) IOP Con. Series: Material Science and Engineering 73 (2015) 012041.

**Figure Captions:**

1. a) XRD pattern of the GeSe<sub>5</sub> chalcogenide glasses, and b) EDX chart.
2. Frequency dependence of  $\sigma_{ac}$  for GeSe<sub>5</sub> at different temperature.
3. Temperature dependence of frequency exponent s.
4. Temperature dependence of  $\sigma_{ac}$  for GeSe<sub>5</sub> chalcogenide glasses.
5. The dependence of ac activation energy on frequency.
6. The dependence on  $\ln(\sigma_{ac} T)$  against  $1000/T$ .
7. a) Frequency dependence of the dielectric constant for GeSe<sub>5</sub> chalcogenide glasses at different temperatures, and b) Temperature dependence of dielectric constant at different frequencies
8. a) Frequency dependence of dielectric loss of GeSe<sub>5</sub> at different temperatures, and b) Temperature dependence of dielectric loss at different frequencies.
9. Frequency dependence of real electric modulus  $M_1$  of GeSe<sub>5</sub> chalcogenide glasses at different temperatures.
10. Frequency dependence of imaginary electric modulus  $M_2$  of GeSe<sub>5</sub> chalcogenide glasses at different temperatures.